Non-linear Velocity Aided Attitude Estimation and Velocity Control for Quadrotors

Moses Bangura, Frits Kuipers, Guillaume Allibert, Robert Mahony

Non-linear Velocity Aided Attitude Estimation and Velocity Control for Quadrotors

Moses Bangura[1], Frits Kuipers[2], Guillaume Allibert[3] and Robert Mahony[1,*]
[2]University of Twente {f.p.kuipers@student.utwente.nl}
[3]University of Nice Sophia Antipolis {Allibert@i3s.unice.fr}
[1]Australian National University, Canberra, Australia {Moses.Bangura, Robert.Mahony}@anu.edu.au

Abstract

In this paper, we present a coupled inertial and body-fixed frame non-linear complementary velocity aided attitude filter and a linear velocity controller for quadrotors. The coupled observers provide estimates of attitude and the different velocities associated with quadrotor motion. With the estimated body-fixed frame velocity, we propose a velocity controller and show that the resulting error dynamics are asymptotically stabilised by the controller. The observer-controller scheme is exploited using an external interface to an android based phone that enables human interaction with the quadrotor. Results of the velocity aided attitude observer compared to ground truth Vicon measurements are presented to illustrate the effectiveness of the estimation scheme. Results of using the android based phone application in setting the desired velocities to illustrate the tracking performance of the controller are also presented.

1 Introduction

Quadrotors as the name implies are aerial vehicles with a four motor-rotor system used for control and generation of thrust [Lim *et al.*, 2012]. The general estimation and control of these vehicles has been done in a hierarchical manner with position and velocity at the top, attitude at the middle and motor thrust control at the lowest level.

Ignoring the motor thrust control, estimators for quadrotors can be grouped into attitude, velocity and position and the more recent combined estimation for attitude and linear velocity. The most common of these is the attitude observer of which there are many different types including Kalman filter based which are the most popular on the majority of open-source quadrotors [Lim *et al.*, 2012], the Left-Invariant Extended Kalman Filter (LIEKF) [Bonnabel, 2007] and the non-linear complementary filters [Mahony *et al.*, 2008]. Unlike the extended Kalman filters, complementary filters take into account the non-linear model of the vehicle. The major disadvantage of doing attitude only estimation is that it requires additional filters for velocity and/or position.

Hence in recent years people have proposed combining the attitude and velocity in a more efficient estimation scheme referred to as velocity aided attitude estimation [Allibert *et al.*, 2014]. Bonnabel [Bonnabel *et al.*, 2009] proposed an invariant extended Kalman filter (EKF) for velocity and attitude estimation in quaternions. Abeywardena and Leishman used an Euler angle based combined roll and pitch and translational velocities with an extended Kalman filter (EKF) [Abeywardena *et al.*, 2013; Leishman *et al.*, 2014]. However, Leishman [Leishman *et al.*, 2014] showed that a drag-force linear fixed-gain (DFFG) filter is the most practical for onboard implementation of such a filter. This high rate estimated velocity and attitude has been exploited and shown to be good for human-quadrotor interaction in the AR. Drone technology [Bristeau *et al.*, 2011].

Similar to the other types of observers, velocity and position filters are usually extended Kalman filter (EKF) based [Briod *et al.*, 2013; Grzonka *et al.*, 2012] though some authors have proposed the use of complementary filters [Sa and Corke, 2012], [Cheviron *et al.*, 2007]. These observers usually couple optical flow [Briod *et al.*, 2013] measurements or simultaneous localisation and mapping (SLAM) [Grzonka *et al.*, 2012] or vision sensors [Cheviron *et al.*, 2007] with onboard inertial sensors to do position and velocity estimation.

In this paper, we present a coupled inertial and body-fixed frame velocity aided attitude observer for quadrotors. Using the drag force model, the measurements of the body-fixed frame linear translational velocities are made. Using either global positioning system (GPS) or a high accuracy motion capture system such as Vicon [VICON Team, 2015], measurements of the inertial frame linear velocities are made. With these and onboard inertial measurements obtained from an inertial measurement unit (IMU) and a magnetometer, two sets of non-linear complementary filters in the inertial and body-fixed frames are proposed. With this approach, esti-

[*]Also with ARC Centre of Excellence for Robotic Vision.

mates of the vehicle velocity in the body-fixed and inertial frames are made as well as an estimate of the wind velocity and the attitude of the vehicle. With these velocities, one can carry out indoor and outdoor flights with/without external sensors such as GPS and Vicon. The two filters are made to converge using coupled innovation terms in both filters. With the estimated velocity at the same frequency as the attitude, we propose a velocity controller along with an autonomous/semi-autonomous control architecture that enables human-quadrotor interaction with an android based phone. Using Lyapunov analysis, we prove local asymptotic stability of the velocity controller on the resulting quadrotor error dynamics. We demonstrate the velocity aided attitude observer using Vicon measurements available on the vehicle at 40Hz as input and the resulting 200Hz estimates of attitude and velocity from the observer in the proposed velocity controller. Velocity and attitude results of the inertial frame filter compared to ground truth measurements from Vicon are presented. The desired (set by pilot using the mobile phone) and estimated velocities are also presented to illustrate the tracking performance of the controller. The different software for the observers and controller that are part of the avionics system are implemented on the PX4 autopilot [Meier *et al.*, 2015]. The avionics software along with the ground station software are available as open-source.

The remainder of the paper is organised as follows: the non-linear quadrotor model is described in Section 2; the proposed velocity aided attitude observer is described in Section 3 and in Section 4, we present the proposed velocity controller. The software architecture framework for the observer and controller scheme is described in Section 5 and in Section 6, we present experimental results of the observer and controller.

2 NON-LINEAR QUADROTOR MODEL

This section describes the non-linear quadrotor model used in the development of the velocity aided attitude observer and the velocity controller described in later sections of the paper.

To present the non-linear model, consider Figure 1 which has an inertial frame denoted $\{A\}$ and a body-fixed frame $\{B\}$. If the mass of the quadrotor is m, g, acceleration due to gravity and T is the total thrust or heave force, $v \in \mathbb{R}^3$ is the velocity of the vehicle in $\{A\}$ and $R \in \mathrm{SO}(3)$ is the rotation matrix from $\{B\}$ to $\{A\}$, $D \in \mathbb{R}^3$ is the drag force expressed in $\{B\}$, and $\Omega \in \mathbb{R}^3$ is the angular velocity of the vehicle in inertial frame, then the linear kinematic model in $\{A\}$ is given by [Bangura and Mahony, 2012]

$$\dot{v} = g\vec{e}_3 - \frac{T}{m}R\vec{e}_3 + \frac{1}{m}RD, \tag{1a}$$

$$\dot{R} = R\Omega_\times. \tag{1b}$$

If $V = R^\top v$ is the velocity of the vehicle in the body-fixed frame, then (1) expressed in $\{B\}$ is

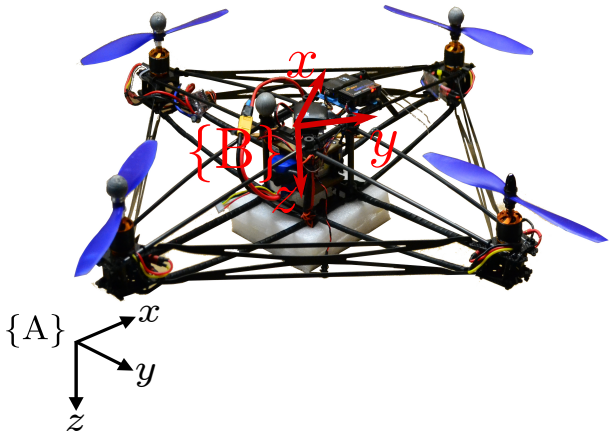

Figure 1: **Quadrotor platform:** The platform used for the experiments showing the body-fixed $\{B\}$ and inertial $\{A\}$ frames. The PX4 is mounted along with the battery on a spring damper system to minimise vibration on IMU measurements.

$$\dot{V} = -\Omega \times V - \frac{T}{m}\vec{e}_3 + gR^\top\vec{e}_3 + \frac{D}{m}, \tag{2a}$$

$$\dot{R} = R\Omega_\times, \tag{2b}$$

where $\Omega_\times \in \mathbb{R}^{3\times 3}$ is the skew symmetric matrix. It is such that $\Omega_\times w = \Omega \times w$ for all $w \in \mathbb{R}^3$. In the sequel, $\vec{e}_1, \vec{e}_2, \vec{e}_3 \in \mathbb{R}^3$ are used to denote unit vectors in x, y and z directions respectively.

We model the drag force $D = -TK_rV \in \{B\}$ and the drag coefficient matrix by [Bangura and Mahony, 2014]

$$K_r = \begin{pmatrix} \bar{c} & 0 & 0 \\ 0 & \bar{c} & 0 \\ 0 & 0 & 0 \end{pmatrix},$$

where $\bar{c} > 0$ is the drag coefficient. Substituting the drag model into (2), one has

$$\dot{V} = -\Omega \times V - \frac{T}{m}\vec{e}_3 + gR^\top\vec{e}_3 - \frac{T}{m}K_rV, \tag{3a}$$

$$\dot{R} = R\Omega_\times. \tag{3b}$$

If the accelerometer measurement is $\bar{a}$, and it measures the external forces, then

$$\bar{a} = -\frac{1}{m}\begin{pmatrix} D \\ T \end{pmatrix},$$

given that $D^\top\vec{e}_3 = 0$. Hence $T = m\bar{a}^\top\vec{e}_3$, which implies that

$$\bar{a}_x = \bar{a}_z\bar{c}V_x, \tag{4a}$$

$$\bar{a}_y = \bar{a}_z\bar{c}V_y. \tag{4b}$$

These equations will be key in computing the measured translational linear velocities in $\{B\}$.

3 VELOCITY AIDED ATTITUDE OBSERVER

In this section, we propose a coupled velocity aided attitude filter in the body-fixed and inertial frames for a quadrotor vehicle. In each of the reference frames is a complementary filter which estimates the velocity of the vehicle and its attitude $\hat{R} \in SO(3)$ in that reference frame. The body-fixed frame $\{B\}$ filter relies on the estimated aerodynamic power $\hat{P}_a$ from the motor-rotor system, inertial measurement unit (IMU) measurements and a drag force model to provide full body-fixed frame measurements of velocity [Allibert *et al.*, 2014]. With these measurements, estimates of the vehicle velocity in $\{B\}$ $\hat{V}$ are made. Parallel to this is a second filter in the inertial frame $\{A\}$ which uses either GPS or Vicon measurements to provide estimates of the vehicle velocity $\hat{v}$ in inertial frame $\{A\}$ and attitude $\hat{R}$. The two filters are made to converge using coupled innovation terms and they output an estimate of the wind velocity. The proposed framework for the coupled inertial and body-fixed frame filters are shown in Figure 2. It should be noted that if v, V are the actual velocities and $\bar{v}, \bar{V}$ are the measured velocities, in this work, we assume that they are the same i.e. $v = \bar{v}$ and $V = \bar{V}$.

Strap down IMUs on quadrotors have a 3-axis gyroscope and a 3-axis accelerometer for measuring angular velocity $\bar{\Omega}$ and the specific acceleration $\bar{a} \in \{B\}$ respectively which are used as inputs to the two filters. A quadrotor equipped with a barometer can also be used to provide measurements of $\bar{v}^\top \vec{e}_3$ that can be used to provide $\bar{V}_z$ and thus the full body fixed frame measurements. Unfortunately, barometers are known to drift and are affected greatly by frequent changes in aerodynamics such as air conditioning and opening/shutting of doors in the indoor experiments carried out in this paper. We assume that the vehicle is equipped with a 3-axis magnetometer which measures the magnetic field $\bar{\mu}$. Unlike [Bangura *et al.*, 2014] which used the raw magnetic field measurements as vectorial measurements, we decouple the roll and pitch so that the magnetometer only gives information on yaw. Furthermore, to remove any magnetic effects of currents caused by motor-rotor load at high rotor speeds, we use a calibration scheme performed offline using current and magnetometer measurements. The magnetic effects of the electric currents are then subtracted from the raw $\bar{\mu}$ measurements with current measurements read from the ESCs via I2C at 20Hz. If $\mathring{\mu} \in \mathbb{R}^3$ is the earth's magnetic field measured in $\{A\}$, and R is the attitude of the vehicle, then the decoupled estimated magnetic field is

$$\hat{\mu} = \hat{R}^\top \mathring{\mu}.$$

We define the operator $\mathbb{P}_a$ to denote the anti-symmetric projection operator in square matrix space by

$$\mathbb{P}_a(H) = \frac{1}{2}(H - H^\top). \tag{5}$$

It should be noted that in the sequel, we use $\beta \in \mathbb{R}^3$ to denote the bias in a measurement, subscript 1 and 2 denote internal

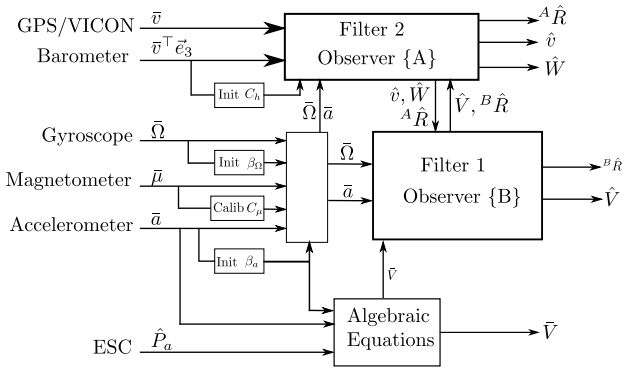

Figure 2: **Overview of the proposed coupled complementary filters:** With GPS/Vicon used to generate velocity measurements for Filter 2 and an algebraic process that uses the estimated aerodynamic power $\hat{P}_a$ to obtain the drift free velocity for Filter 1 and onboard IMU and magnetometer measurements, the different velocities and attitude of the vehicle are estimated by the proposed observers. It should be noted that the attitudes determined by the two filters converge as a result of the coupling innovation terms i.e. ${}^A R = {}^B R$.

variables used by Filter 1 in $\{B\}$ and Filter 2 in $\{A\}$ respectively. If we assume that the trajectory of the quadrotor is smooth with $\Omega(t), \dot{\Omega}(t), v(t), \dot{v}(t), V(t)$ and $\dot{V}(t)$ bounded, we propose without proof the following observers.

For the filter in the body-fixed frame $\{B\}$ (Filter 1), we propose the following.

Theorem 1. *Let $k_1^{vc}, k_1^r, k_1^\mu, k_1^{\beta a}$ be positive scalar gains with measurements $\bar{\Omega}, \bar{a}, V = \bar{V}$ and $\bar{\mu}$, then consider the observer*

$$\dot{\hat{V}}_1 = -(\bar{\Omega} - \hat{\beta}_1^\Omega)_\times \hat{V}_1 + g X_1^\top \vec{e}_3 + (\bar{a} - \hat{\beta}_1^a) - \Delta_1^v - k_1^{vc} \Delta_1^{vc}, \tag{6a}$$

$$\dot{X}_1 = \dot{u}_1 \hat{R}_1 + u_1 \dot{\hat{R}}_1, \tag{6b}$$

$$\dot{\hat{R}}_1 = \hat{R}_1 (\bar{\Omega} - \hat{\beta}_1^\Omega)_\times - k_1^r \Delta_{1\times}^r \hat{R}_1 + \hat{R}_1 \Delta_1^\mu - \Delta_1^{rc} \hat{R}_1, \tag{6c}$$

$$\dot{u}_1 = -k_1^\mu g \tilde{V}_1^\top \hat{R}_1^\top \vec{e}_3, \tag{6d}$$

$$\dot{\hat{\beta}}_1^a = k_1^{\beta a} \Delta_1^v - k_1^{\beta ac} (\hat{\beta}_1^a - \hat{\beta}_2^a), \tag{6e}$$

$$\dot{\hat{\beta}}_1^\Omega = k_1^{\beta\Omega} \Delta_1^r, \tag{6f}$$

where $\tilde{V} = \hat{V} - V$, $X = u\hat{R}$ is the scaled rotation and the upper triangular orthogonal decomposition of X with u a positive scalar. The initial conditions are $\hat{V}_1(0) = V_1(0)$, $X_1(0) = u_1(0)\hat{R}_1(0)$, $u_1(0) = 1$, $\hat{R}_1(0) = I$ and I is the identity matrix. We define the innovations $\Delta_1^v, \Delta_1^r, \Delta_1^\mu$ by

$$\Delta_1^v = k_1^v (\hat{V}_1 - V_1), \tag{7a}$$

$$\Delta_1^r = \frac{g}{u_1} \hat{R}_1 \tilde{V}_1 \times \vec{e}_3, \tag{7b}$$

$$\Delta_1^\mu = k_1^\mu (((\bar{\mu} \times \hat{\mu})^\top X_1^\top \vec{e}_3) X_1^\top \vec{e}_3)_\times, \tag{7c}$$

and the coupling innovation terms Δ_1^{vc} and Δ_1^{rc} by

$$\Delta_1^{vc} = \hat{V}_1 - \hat{R}_1^\top(\hat{v}_2 - \hat{W}), \tag{8a}$$

$$\Delta_1^{rc} = k_1^{rc}\mathbb{P}_a(\hat{R}_1\hat{R}_2^\top), \tag{8b}$$

then for almost all initial conditions, $\hat{V}_1(t) = V_1(t)$ and $\hat{R}_1(t) = R_1(t)$.

For the inertial frame filter i.e. Filter 2, we propose the following complementary filter.

Theorem 2. *Consider the model* (1) *in the $\{A\}$ frame of reference with measurements $\bar{a}$, $\bar{\Omega}$ and $v = \bar{v}$. Let $k_2^r, k_2^u, k_2^w, k_2^{\beta a}, k_2^v$ be positive scalar gains, then consider the observer*

$$\dot{\hat{v}}_2 = \hat{R}_2(\bar{a} - \hat{\beta}_2^a) + g\vec{e}_3 - \Delta_2^v - \Delta_2^{vc}, \tag{9a}$$

$$\dot{\hat{R}}_2 = \hat{R}_2(\bar{\Omega} - \hat{\beta}_2^\Omega)_\times - k_2^r\Delta_{2\times}^r\hat{R}_2 - \Delta_2^{rc}\hat{R}_2, \tag{9b}$$

$$\dot{u}_2 = -k_2^u g\tilde{v}_2^\top\vec{e}_3, \tag{9c}$$

$$\dot{\hat{W}} = -k_2^w\left((\hat{W} - \hat{v}_2) + \hat{R}_1\hat{V}_1\right), \tag{9d}$$

$$\dot{\hat{\beta}}_2^a = k_2^{\beta a}\Delta_2^v - k_2^{\beta ac}(\hat{\beta}_2^a - \hat{\beta}_1^a), \tag{9e}$$

$$\dot{\hat{\beta}}_2^\Omega = k_2^{\beta\Omega}\Delta_2^r, \tag{9f}$$

with initial conditions $\hat{v}_2(0) = v_2(0)$, $u_2(0) = 1, \hat{W}(0) = W(0), \hat{R}_2(0) = I$ and $\tilde{v} = \hat{v} - v$. The innovations Δ_2^v and Δ_2^r are given by

$$\Delta_2^r = \frac{g}{u_2}\tilde{v}_2 \times \vec{e}_3, \tag{10a}$$

$$\Delta_2^v = k_2^v(\hat{v}_2 - v). \tag{10b}$$

The coupling innovation terms Δ_2^{vc} and Δ_2^{rc} are given by

$$\Delta_2^{vc} = k_2^{vc}\left((\hat{v}_2 - \hat{W}) - \hat{R}_1\hat{V}_1\right), \tag{11a}$$

$$\Delta_2^{rc} = k_2^c\mathbb{P}_a\left(\hat{R}_2\hat{R}_1^\top\right), \tag{11b}$$

then for almost all initial conditions, $\hat{v}_2(t) \to v_2(t)$, $\hat{W}(t) \to W(t)$ and $\hat{R}_2(t) \to R_2(t)$.

Ignoring the coupling terms, the convergence proof for Theorem 1 is presented in the authors' previous work [Allibert *et al.*, 2014]. Theorem 2 can also be proven using a similar approach. In Section 6, we present experimental results of flying in a high accuracy motion capture environment to illustrate convergence of the two filters.

With $\bar{v}_2$ measurements provided by either GPS or Vicon [VICON Team, 2015] and $\bar{V}_1$ computed based on (4) and rotated $\bar{v}$ in $\vec{e}_3$ direction, then $\hat{V}$ can be estimated from Filter 1 $\{B\}$ and $\hat{v}$ from Filter 2 and the wind velocity $\hat{W} \in \{A\}$ can also be estimated. Hence the proposed coupled complementary filters can be used to provide estimates of the vehicle attitude $\hat{R}$ and velocities $\hat{v}, \hat{V}, \hat{W}$ that will enable autonomous/semi-autonomous indoor and outdoor flights of quadrotors.

4 VELOCITY CONTROLLER

In this section, we present the theoretical development of the velocity controller for precise tracking of velocity setpoints. We use the derivative of the position of the well known differential flat outputs (x, y, z, ψ) in the body-fixed frame $\{B\}$ i.e. $(\dot{x}, \dot{y}, \dot{z}, \psi)$ rotated to $\{B\}$ and exploit the passivity of the system to prove local asymptotic stability using Lyapunov analysis for the velocity error dynamics under the proposed control law. The outputs of the controller are the desired attitude in quaternion and the total or heave force which are regulated by the middle and low-level controllers in Bangura *et. al.* [Bangura *et al.*, 2014]. This development will not use Euler angles as they suffer from ambiguity and gimbal lock. Furthermore, for different desired velocities, the associated yaw will be physically a different orientation. As such, a desired orientation in $\vec{e}_1$ direction in frame $\{A\}$ is specified, so that if the desired orientation is $\eta \in \mathbb{R}^3$ in $\vec{e}_1$ in $\{B\}$, it is given by

$$\eta = R_3^\top(\psi)\vec{e}_1 = \begin{bmatrix}\cos\psi & -\sin\psi & 0\end{bmatrix}^\top, \tag{12}$$

where R_3 is the rotation matrix about the $\vec{e}_3$ direction.

4.1 Model Reduction

From Section 2, the drag force can be written as [Bangura and Mahony, 2014]

$$TK_rV = T\bar{c}V - T\bar{c}V_z\vec{e}_3.$$

Using $\bar{T} = T(1 - \bar{c}V_z)$, (3a) becomes [Omari *et al.*, 2013]

$$\dot{V} = -\Omega \times V + gR^\top\vec{e}_3 - \frac{\bar{T}}{m}\vec{e}_3 - \frac{T}{m}\bar{c}V. \tag{13}$$

Knowing that there are unmodelled dynamics, we add $\delta \in \mathbb{R}^3$ to model the constant error in the model. Hence, (13) can be written as

$$\dot{V} = -\Omega \times V + gR^\top\vec{e}_3 - \frac{\bar{T}}{m}\vec{e}_3 - \frac{T}{m}\bar{c}V + \delta.$$

The constant error ($\delta \in \mathbb{R}^3$) will be dealt with by the integral action of the controller.

4.2 Velocity Controller

Let the desired velocity be $V^d \in \mathbb{R}^3$ and the desired acceleration $\dot{V}^d = 0$, then the velocity error $\tilde{V} = V - V^d$ with error dynamics is given by

$$\dot{\tilde{V}} = -\Omega \times V + gR^\top\vec{e}_3 - \frac{\bar{T}}{m}\vec{e}_3 - \frac{T}{m}\bar{c}V + \delta - \dot{V}_d. \tag{14}$$

Based on time-scale separation of the different dynamic levels of a quadrotor that have been shown to be hierarchical in structure, we make the following assumptions [Bangura *et al.*, 2014; Bangura and Mahony, 2014]

Assumption 1. *1. The attitude and velocity filters have converged so that $\hat{R}(t) = R(t)$ and $\hat{V}(t) = V(t)$.*

2. *The attitude controller is fast and has reached its desired value such that* $\forall t$, $R_d(t) = R(t)$ *or in quaternion* $q_d(t) = q(t)$.
3. *The motor controllers are such that within the time constant of the velocity controller, for all time* t, $T_d(t) = T(t)$.

Based on Assumption 1, we propose the following theorem.

Theorem 3. *Let the desired bounded velocity be* $V^d \in \mathbb{R}^3$ *and the desired acceleration* $\dot{V}^d = 0$ *in* $\{B\}$. *Let* $K_i, K_p \in \mathbb{R}^{3\times3}$ *be positive definite gain matrices and consider the following condition for the desired attitude* R_d

$$mgR_d^\top \vec{e}_3 = \bar{T}_d\vec{e}_3 + T_d\bar{c}V_d + m\Omega\times V_d - mK_p\tilde{V} - m\hat{\delta}, \quad (15a)$$

$$\dot{\hat{\delta}} = K_i\tilde{V},\ \hat{\delta}(0) = \hat{\delta}_0, \quad (15b)$$

where $\hat{\delta} \in \mathbb{R}^3$ *is bounded and is an estimate of the model error* δ *and* $\hat{\delta}_0$ *is some initial condition. Then the error dynamics of* (14) *are locally asymptotically stable (LAS) around the equilibrium* $\tilde{V} = 0$.

Proof. Substituting the controller (15a) into the error dynamics (14) with $\dot{V}_d = 0$ and invoking Assumption 1,

$$\dot{\tilde{V}} = -\Omega\times\tilde{V} - \frac{T}{m}\bar{c}\tilde{V} - K_p\tilde{V} + \tilde{\delta},$$

where $\tilde{\delta} = \delta - \hat{\delta}$ and $\dot{\tilde{\delta}} = -\dot{\hat{\delta}}$, given $\dot{\delta} = 0$. Thus the system of equations for the new error dynamics are

$$\dot{\tilde{V}} = -\Omega\times\tilde{V} - \frac{T}{m}\bar{c}\tilde{V} - K_p\tilde{V} + \tilde{\delta}, \quad (16a)$$

$$\dot{\tilde{\delta}} = -\dot{\hat{\delta}}. \quad (16b)$$

To prove stability of (16), consider the following Lyapunov function

$$\mathscr{L} = \frac{1}{2}\tilde{V}^\top\tilde{V} + \frac{1}{2}\tilde{\delta}^\top K_i^{-1}\tilde{\delta}, \quad (17)$$

which is positive definite. Taking the derivative of (17),

$$\begin{aligned}\dot{\mathscr{L}} &= \tilde{V}^\top\dot{\tilde{V}} + \tilde{\delta}^\top K_i^{-1}\dot{\tilde{\delta}},\\ &= \tilde{V}^\top\left(-\Omega\times\tilde{V} - \frac{T}{m}\bar{c}\tilde{V} - K_p\tilde{V} + \tilde{\delta}\right) + \tilde{\delta}^\top K_i^{-1}(-\dot{\hat{\delta}}),\\ &= \tilde{V}^\top\left(-\Omega\times\tilde{V} - \frac{T}{m}\bar{c}\tilde{V} - K_p\tilde{V}\right) + \tilde{\delta}^\top\left(\tilde{V} - K_i^{-1}\dot{\hat{\delta}}\right).\end{aligned}$$

From Theorem 3,

$$\dot{\mathscr{L}} = \tilde{V}^\top\left(-\Omega\times\tilde{V} - \frac{T}{m}\bar{c}\tilde{V} - K_p\tilde{V}\right).$$

However, $\tilde{V}^\top\Omega_\times\tilde{V} = 0$ and $\forall t\ T(t) > 0$, hence,

$$\dot{\mathscr{L}} = -\tilde{V}^\top\left(\frac{T}{m}\bar{c}I + K_p\right)\tilde{V}. \quad (18)$$

To show that $\dot{\mathscr{L}} \to 0$ with $\tilde{V} \to 0$ as $t \to \infty$, we need to show that $\dot{\mathscr{L}}$ is uniformly continuous. Taking the derivative of (18) yields,

$$\ddot{\mathscr{L}} = -2\tilde{V}^\top\left(\frac{T}{m}\bar{c}I + K_p\right)\left(-\frac{T}{m}\bar{c}\tilde{V} - K_p\tilde{V} + \tilde{\delta}\right). \quad (19)$$

Given that all signals of (19) are bounded demonstrates that (18) is uniformly continuous. Therefore by Barbalat's lemma, $\dot{\mathscr{L}}$ converges to zero thus $\tilde{V} \to 0$ asymptotically. With $\tilde{V} \to 0$, implies that from (15b), $\dot{\tilde{\delta}} \to 0$, hence $\dot{\hat{\delta}} \to \delta$. Therefore, the system (14) is locally asymptotically stable under the control law of (15).

□

Substituting for $\dot{\hat{\delta}}$ using (15b) into the controller of (15a),

$$mgR_d^\top \vec{e}_3 = \bar{T}_d\vec{e}_3 + T_d\bar{c}V_d + m\Omega\times V_d - mK_p\tilde{V} - mK_i\int_0^t \tilde{V}(\tau)\mathrm{d}\tau. \quad (20)$$

To avoid large integral windup, the integral part of the controller (20) is implemented as

$$\dot{\hat{\delta}} = -K_\delta\hat{\delta} + K_i\mathrm{Sat}^\Delta\left(\tilde{V} + K_\delta K_i^{-1}\tilde{\delta}\right),$$

where $K_\delta \in \mathbb{R}^{3\times3}$ is a positive definite gain matrix and the bounds of the saturation function $\mathrm{Sat}^\Delta(.) \in \mathbb{R}^3$ are set as desired. It should be noted that $\mathrm{Sat}^\Delta(.) \succ 0$ and its inclusion does not change the proof of Theorem 3 [Hua *et al.*, 2013].

Remark 1. *Note that the controller condition* (15a) *only constrains the desired attitude* R_d *to 2 degrees of freedom. The third degree of freedom can be fixed as desired without changing the proof of Theorem 3.*

To obtain all the elements of the desired attitude R_d, recalling the user specified desired direction η from (12) which is the projection of R_d unto $\{B\}$ in $\vec{e}_1$ direction, if we set the controller output $R_d^\top\vec{e}_3 = \gamma$, if $\chi, \nu \in \mathbb{R}^3$, such that the desired attitude can be written as $R_d^\top = \begin{pmatrix}\chi & \nu & \gamma\end{pmatrix}$ and let $\sigma > 0$ be defined by

$$\sigma = |\gamma\times\eta|.$$

Provided η is not parallel to γ in which case $\sigma = 0$ and using the orthogonal property of $R_d \in \mathrm{SO}(3)$, then

$$\nu = \frac{\gamma\times\eta}{\sigma},$$

$$\chi = \nu\times\gamma.$$

With χ, ν, γ known, hence, $R_d^\top$ is also known. From this R_d, the desired quaternion $q_d \in \mathbb{R}^4$ is then computed. This desired quaternion is then regulated by the inner loop controllers of Bangura *et. al.* [Bangura *et al.*, 2014]. It should be noted that with the coupled observer proposed in Section 3, q_0 of the attitude ($q = (q_0, q_1, q_2, q_3)^\top$) extracted from R is always

positive and therefore there is no need to consider the unwinding problem associated with attitude control in quaternions. Hence $q_{d_0} > 0$. Unlike the proportional $\Omega^\top \vec{e}_3$ controller of [Bangura *et al.*, 2014], we use a *PI* controller to achieve our desired $\tilde{\Omega}^\top \vec{e}_3 = 0$ objective. From the experimental results, the dynamic effect of the integral does not affect the overall stability of the system as it is decoupled from the translational and vertical dynamics.

From the controller (20), the desired thrust is computed using

$$T_d = mg\left(|R^\top \vec{e}_3 \vec{e}_3^\top|\right) - m\left(\Omega \times V_d\right)^\top \vec{e}_3 + \left(mK_p\tilde{V} + mK_i\int_0^t \tilde{V}(\tau)\mathrm{d}\tau\right)\vec{e}_3.$$

In manual mode operation of a quadrotor using stick inputs from an RC transmitter, the stick channels are such that the desired attitude and thrust $(\phi^d, \theta^d, T^d, \dot{\psi}^d)$ correspond to channels 1 to 4 of the transmitter respectively. In a similar manner we match the desired velocities to the respective channels as $(v_y^d, v_x^d, T^d, \dot{\psi})$. To ensure that the desired velocity is in the same frame as the pilot such that the vehicle response to stick inputs are similar to those of roll and pitch control, we propose a third frame of reference denoted $\{C\}$ for the desired velocities. This frame is equivalent to the inertial frame $\{A\}$ with its $\vec{e}_1$ direction aligned with the vehicle's $\vec{e}_1$ direction.

5 ARCHITECTURE

In this section, we describe the architecture along with the various applications including the observer and controller and how they interact on the PX4 autopilot. The section also describes how the vehicle connects to a ground station computer using our open-source codes. As an example of an external device that can be used with the architecture to enable human-quadrotor interaction is an android phone. The phone is used to control the vehicle and thus provide desired velocity and orientation setpoints.

5.1 Ground Station

The ground station consists of a Linux based computer with a set of software running on the Robot Operating System (ROS) [Quigley *et al.*, 2009]. It communicates with the quadrotor using a 915MHz 3DR radio. From the ground station, the desired velocity and yaw (V^d, ψ^d) are sent to the vehicle. Please note that the desired orientation is computed using (12). If Vicon data is available, the position ζ, and attitude R_v measurements are also sent and received on the PX4 at a hardware limited rate of 40Hz.

The ground station has a finite state machine that takes inputs from a user through a terminal. In the state machine, the input is an integer (0 - 99) that corresponds to a particular hard coded trajectory/path which the trajectory generator listens to and produces. Within the trajectory generator, additional states can be created with new message types that correspond to new desired trajectories or a waypoint. Examples

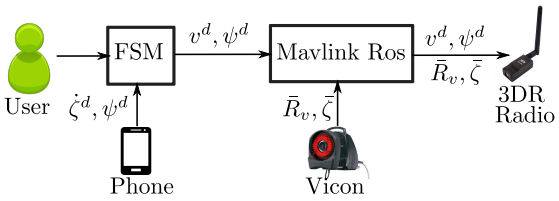

Figure 3: **Simplified ground station architecture:** The simplified diagram shows the finite state machine, the phone, Vicon and the transmitted data to the vehicle through the 3DR radio.

of such states include those that listen to devices such as mobile phones, game consoles, haptic devices etc. A simplified diagram of the ground station is shown in Figure 3.

5.2 Mobile Phone Application

An example of a trajectory $\left(\zeta^d = 0, v^d, \dot{v}^d = 0, \psi^d\right)$ generating application that can be used with the ground station/quadrotor system is a mobile phone application. The phone application developed produces a custom ROS message which the trajectory generator reads whenever the user sets the state machine to use phone messages. The android based phone application enables the phone to communicate with the ground station through a WiFi internet connection using web sockets. The graphical user interface (GUI) of the phone which the user interacts with is shown in Figure 4. As shown in the figure, the application has other functionalities such as hover and land the vehicle at the current x, y, ψ or do position control when position data is available on the vehicle. The application on the phone was used to generate the desired velocities for Section 6.

5.3 Avionics

The velocity aided attitude estimation along with the velocity and attitude controllers were implemented on the PX4 autopilot. The PX4 open-source software architecture is modular and uses a publish-subscribe object request paradigm in a multi-threaded framework on the NuttX real-time operating system [Meier *et al.*, 2015]. This makes it possible to add new applications and object types.

The PX4FMU/IO hardware is equipped with the 3-axis Honeywell HMC5883L magnetometer, an INVENSENSE MPU-6000 inertial measurement unit (IMU) that consists of a 3-axis gyroscope and a 3-axis accelerometer. It also has a highly sensitive MS5611-01BA03 pressure sensor barometer with an accuracy of 10cm for measuring altitude.

Attached to the PX4 is an RC receiver which allows for manual control (channels 1 to 4) and for mode switching from manual to autonomous using channel 5.

The software architecture onboard the autopilot is shown in Figure 5. mc_quat_pos_control implements the generation of the measured velocities in the inertial frames $\bar{v}_2$ using external sensors such as Vicon motion system or GPS.

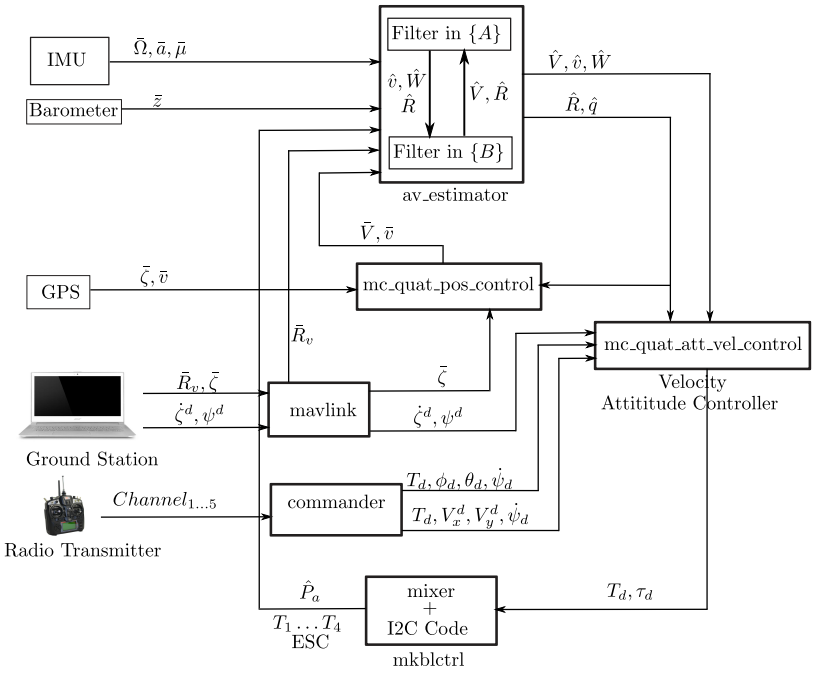

Figure 5: **Proposed Software Architecture:** This is the software implemented for the observer and controller on the PX4 autopilot, ground station, radio transmitter and sensors. In addition, the computed desired torque τ_d from the attitude controller and the estimated aerodynamic power $\hat{P}_a$ are also shown.

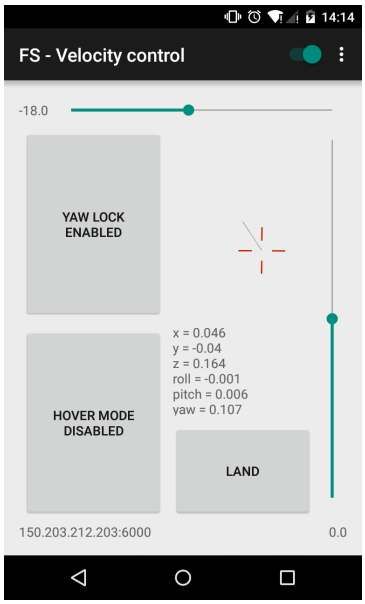

Figure 4: **Screenshot of mobile application on Nexus 5:** Application GUI on phone in velocity control mode with various functionalities and vehicle state (position and attitude). Device rotation in $\vec{e}_1, \vec{e}_2$ maps to desired vehicle velocity in $\vec{e}_1$ and $\vec{e}_2$ directions. $\vec{e}_3$ velocity is set using the right side bar or volume button. Yaw is set by rotating the phone in $\vec{e}_3$ direction or by moving the yaw bar with yaw lock disabled.

The mc_att_vel_controller, implements the velocity controller proposed in Section 4 and the attitude controller of [Bangura *et al.*, 2014]. The av_estimator implements the filters proposed in Section 3 and $\bar{V}$ using rotated $\bar{v}$ for $\vec{e}_3$ measurements and the drag force model. The mavlink application receives mavlink messages (Vicon position and desired trajectory) from the ground station via the 3DR radio. The commander has the magnetometer current calibration and implements the RC signals.

6 EXPERIMENTAL RESULTS

In this section we present experimental results of the observer using input velocities obtained from 40Hz position measurements through Vicon to Filter 2 on the PX4 autopilot along with a comparison of the two attitudes. With the onboard estimated attitude and velocity at 200Hz, the velocity controller is then used to regulate different velocity inputs from a pilot using the android phone with the vehicle in autonomous mode. A similar approach is used in the commercially available AR. Drone [Bristeau *et al.*, 2011]. The resulting tracking performance of the velocity controller is also presented.

6.1 Observer Results

The drag coefficient determination is shown on Figure 6. Using measured $\bar{V}_x$ derived from rotation of $\bar{v}$ from Vicon along with accelerometer measurements, the drag coefficient $\bar{c}$ is determined using linear regression. The obtained $\bar{c}$ is used along with accelerometer measurements to demonstrate the

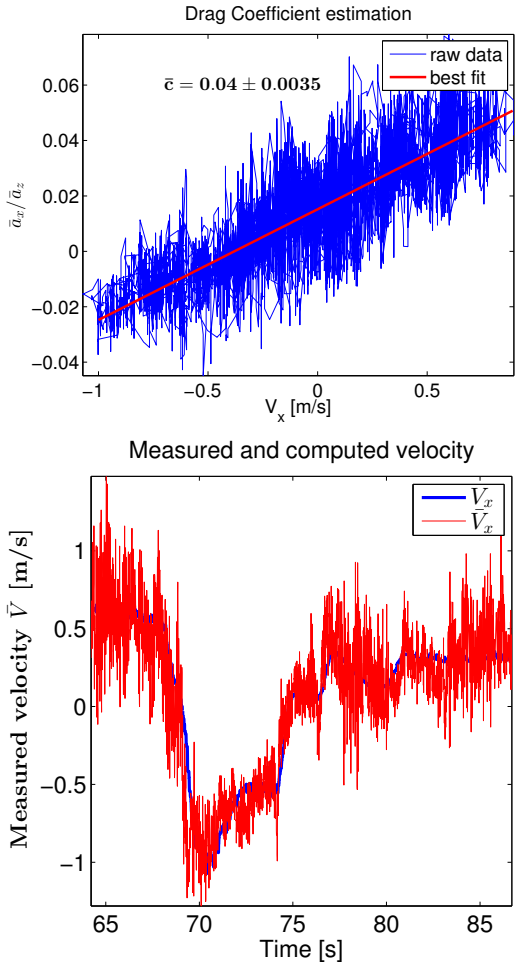

Figure 6: **Drag coefficient $\bar{c}$ determination:** The first plot shows measured accelerometer data $\frac{\bar{a}_x}{\bar{a}_z}$ against measured $\bar{V}_x$ provided by Vicon and the estimated drag coefficient $\bar{c}$ (using (4a)) with its associated line of best fit and 95% confidence interval. Using this $\bar{c}$, and the accelerometer measurements, the second plot shows measured velocity from Vicon (blue) along with the computed velocities obtained using the estimated $\bar{c}$ (red) to demonstrate the quality of the fit. The $\bar{c}$ computed velocities provide the measured translational linear velocities for Filter 1.

quality of the fit in the second plot. The $\bar{c}$ is then used in the algebraic block of Figure 2 to provide measurements of V in $\vec{e}_1$ and $\vec{e}_2$ direction for Filter 1 using (4). To obtain $\bar{V}_z$, the method proposed in [Allibert *et al.*, 2014] can be used. However, this is an ongoing work.

Remark 2. *The rotated Vicon measurement of $\bar{V}_z$ is used as a replacement for the $\bar{V}_z$ measurement in Filter 1 in $\{B\}$. For future work this will be replaced by the $\bar{V}_z$ obtained from the aerodynamic power and thrust model.*

To ensure that the $\vec{e}_1$ direction of the onboard attitude filter aligns with the input $\vec{e}_1$ from Vicon measurements, we pro-

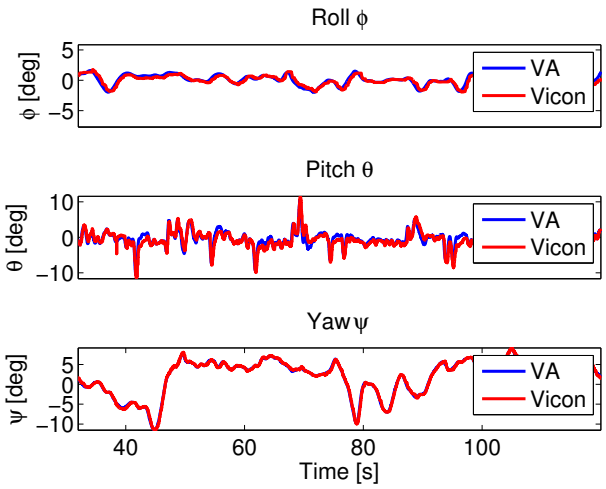

Figure 7: **Filter in $\{\mathbf{A}\}$ Attitude:** Comparison of the attitude estimated by the velocity aided Filter 2 shown in blue to Vicon ground truth measurements shown in red. The results show that the obtained attitude has almost zero error when compared to Vicon measurements.

pose an additional innovation term (21) for Filter 2 in $\{A\}$.

$$\Delta_4 = -k_2^{vicon}\hat{R}_1(e_1 \times \hat{R}_1\hat{R}_v^T e_1)_\times \hat{R}_1. \tag{21}$$

The attitude responses of Filter 2 which equals Filter 1 compared to ground truth measurements by Vicon are shown in Figure 7. The estimated velocity in the inertial frame from Filter 2 along with ground truth from Vicon are shown in Figure 8. The innovation term (21) ensures that the error in yaw between the observer and Vicon is zero. Both the observed attitude and velocity showed almost zero error when compared to ground truth measurements.

6.2 Velocity Controller Results

To demonstrate the tracking performance of the velocity controller, the android phone was used to generate the desired velocities and yaw. The associated quadrotor response, real-time velocity of the vehicle along with the desired velocity displayed on the phone as well as the hand motion of the pilot are presented in the accompanying video. The desired and estimated velocities of the vehicle in $\{A\}$ are shown in Figure 9. The results show that the controller is able to obtain good tracking of the desired velocities.

6.3 Observer Results

Remark 3. *The attitude of the filters are initialised to the initial measurements for fast convergence of the filters. The accelerometer and magnetometer are sampled for half a second and the averaged value is used in the startup sequence to compute this initial measurement. This helps in the estimation of yaw since the true magnetic north might be too far from zero.*

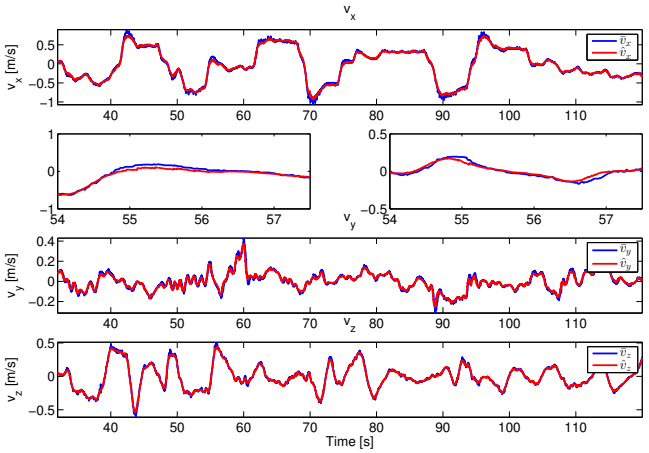

Figure 8: **Velocity estimates of Filter 2 in $\{\mathbf{A}\}$:** The figure shows results of the input velocities from Vicon $\bar{v} \in \{A\}$ shown in blue and the estimated velocities from the filter $\hat{v} \in \{A\}$ shown in red. It is easily seen that the estimated velocity at 200Hz tracks the measured velocities at 40Hz.

It should be noted that the attitude estimation will still work in the absence of GPS or Vicon velocity measurements. This is achieved by setting the coupling innovation terms Δ_1^{vc} and Δ_1^{rc} to 0 in Filter 1 and $\Delta_2^{vc} = \Delta_2^{rc} = 0$ in Filter 2. Though there will not be $\hat{v}, \hat{W}$, the estimation process will result in the so called drift free velocity i.e. $\hat{V} \in \{B\}$ [Abeywardena *et al.*, 2013].

7 CONCLUSION AND FUTURE WORK

In this paper, we have presented results for a proposed coupled non-linear complementary velocity aided attitude filter and a velocity controller for quadrotors. The two filters (body-fixed and inertial frames) both estimate separately the attitude and velocities of the vehicle. Combining the two by the use of coupling innovation terms, which make the filters to converge also enables the estimation of the wind velocity. The estimated body-fixed frame velocity is then used with a proposed velocity controller to track desired velocity setpoints specified by a mobile phone used as a human-quadrotor interface. We proved local asymptotic stability of the proposed controller in tracking a desired velocity setpoint using Lyapunov analysis. The results of the estimated attitude and velocity compared to ground truth Vicon measurements showed good performance of the proposed filters. Furthermore, the velocity controller also showed good tracking performance and thus enables the vehicle to be flown with ease by anyone.

ACKNOWLEDGEMENT

This research was supported by the Australian Research Council through Discovery Grant DP120100316 “Integrated

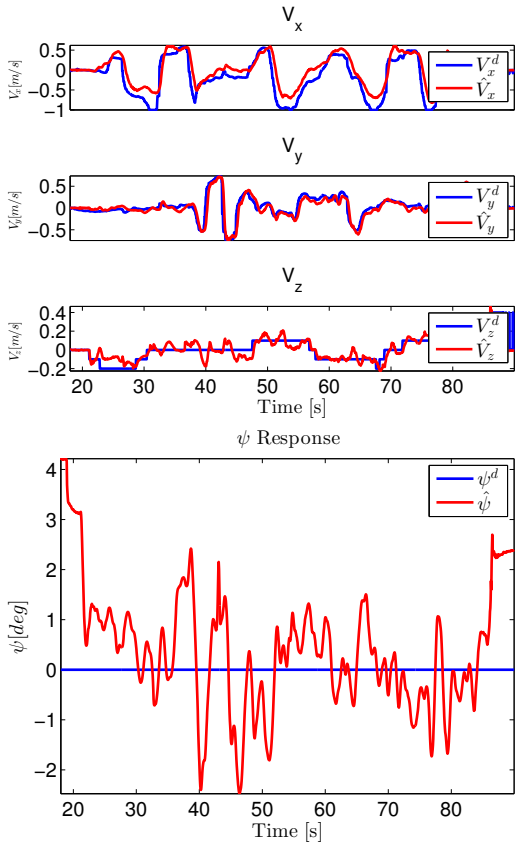

Figure 9: **Velocity controller results:** The results for tracking reference velocity setpoints and orientation (blue) along with estimated velocities and yaw responses of the vehicle (red). The tracking errors are very small for linear velocities and desired orientation and therefore the controller achieved its desired purpose.

High-Performance Control of Aerial Robots in Dynamic Environments” and the ANR-Equipex project “Robotex”.

References

[Abeywardena *et al.*, 2013] Dinuka Abeywardena, Sarath Kodagoda, Gamini Dissanayake, and Rohan Munasinghe. Improved state estimation in quadrotor mavs: A novel drift-free velocity estimator. *Robotics Automation Magazine, IEEE*, 20:32–39, 2013.

[Allibert *et al.*, 2014] Guillaume Allibert, Dinuka Abeywardena, Moses Bangura, and Robert Mahony. Estimating body-fixed frame velocity and attitude from inertial measurements for a quadrotor vehicle. In *Control Applications (CCA), 2014 IEEE Conference on*, pages 978–983. IEEE, 2014.

[Bangura and Mahony, 2012] Moses Bangura and Robert Mahony. Nonlinear dynamic modeling for high perfor-

mance control of a quadrotor. In *Australasian Conference on Robotics and Automation*, 2012.

[Bangura and Mahony, 2014] Moses Bangura and Robert Mahony. Real-time model predictive control for quadrotors. In *IFAC World Congress*, 2014.

[Bangura *et al.*, 2014] Moses Bangura, Hyon Lim, H. Jin Kim, and Robert Mahony. An open-source implementation of a unit quaternion based attitude and trajectory tracking for quadrotors. In *Australasian Conference on Robotics and Automation*, 2014.

[Bonnabel *et al.*, 2009] Silvere Bonnabel, Philippe Martin, and Erwan Salaün. Invariant extended kalman filter: theory and application to a velocity-aided attitude estimation problem. In *Decision and Control, 2009 held jointly with the 2009 28th Chinese Control Conference. CDC/CCC 2009. Proceedings of the 48th IEEE Conference on*, pages 1297–1304. IEEE, 2009.

[Bonnabel, 2007] Silvere Bonnabel. Left-invariant extended kalman filter and attitude estimation. In *IEEE conference on decision and control*, pages 1027–1032, 2007.

[Briod *et al.*, 2013] Adrien Briod, Jean-Christophe Zufferey, and Dario Floreano. Optic-flow based control of a 46g quadrotor. In *Workshop on Vision-based Closed-Loop Control and Navigation of Micro Helicopters in GPS-denied Environments, IROS 2013*, number EPFL-CONF-189879, 2013.

[Bristeau *et al.*, 2011] Pierre-Jean Bristeau, François Callou, David Vissiere, and Nicolas Petit. The navigation and control technology inside the ar. drone micro uav. In *18th IFAC world congress*, volume 18, pages 1477–1484, 2011.

[Cheviron *et al.*, 2007] Thibault Cheviron, Tarek Hamel, Robert Mahony, and Grant Baldwin. Robust nonlinear fusion of inertial and visual data for position, velocity and attitude estimation of uav. In *Robotics and Automation, 2007 IEEE International Conference on*, pages 2010–2016. IEEE, 2007.

[Grzonka *et al.*, 2012] Slawomir Grzonka, Giorgio Grisetti, and Wolfram Burgard. A fully autonomous indoor quadrotor. *Robotics, IEEE Transactions on*, 28(1):90–100, 2012.

[Hua *et al.*, 2013] Minh-Duc Hua, Tarek Hamel, Pascal Morin, and Claude Samson. Introduction to feedback control of underactuated vtol vehicles: A review of basic control design ideas and principles. *IEEE Control Systems magazine*, 33(1), 2013.

[Leishman *et al.*, 2014] Robert C. Leishman, John C. Macdonald, Randal W. Beard, and Timothy W McLain. Quadrotors and accelerometers: State estimation with an improved dynamic model. *Control Systems, IEEE*, 34(1):28–41, 2014.

[Lim *et al.*, 2012] Hyon Lim, Jaemann Park, Daewon Lee, and H. J. Kim. Build your own quadrotor: Open-source projects on unmanned aerial vehicles. *Robotics Automation Magazine, IEEE*, 19(3):33–45, Sept 2012.

[Mahony *et al.*, 2008] Robert Mahony, Tarek Hamel, and Jean-Michel Pflimlin. Nonlinear complementary filters on the special orthogonal group. *Automatic Control, IEEE Transactions on*, 53(5):1203–1218, 2008.

[Meier *et al.*, 2015] Lorenz Meier, Dominik Honegger, and Marc Pollefeys. Px4: A node-based multithreaded open source robotics framework for deeply embedded platforms. *Robotics and Automation, 2015. ICRA'15. IEEE Int. Conference on*, 2015.

[Omari *et al.*, 2013] S. Omari, M.-D. Hua, G. Ducard, and T. Hamel. Nonlinear control of vtol uavs incorporating flapping dynamics. In *IEEE/RSJ Int. Conference on Intelligent Robots and Systems*, page to appear, 2013.

[Quigley *et al.*, 2009] Morgan Quigley, Ken Conley, Brian Gerkey, Josh Faust, Tully Foote, Jeremy Leibs, Rob Wheeler, and Andrew Y Ng. Ros: an open-source robot operating system. In *ICRA workshop on open source software*, volume 3, page 5, 2009.

[Sa and Corke, 2012] Inkyu Sa and Peter Corke. 100hz onboard vision for quadrotor state estimation. In *Australasian Conference on Robotics and Automation*, 2012.

[VICON Team, 2015] VICON Team. Vicon motion systems. "`https://http://www.vicon.com/`", 2015. [Online; accessed 14-June-2015].